Cyclic Plasticity Modeling with ANSYS Mechanical APDL

Abstract
Material modeling and simulation belong to the most exciting areas of contemporary condensed matter physics. This paper is the first in a series of concise yet thorough studies of the physical principles and mathematical concepts underlying a few of the phenomenological material models available in ANSYS Mechanical APDL 12.0.

Assuming a basic background in continuum mechanics, this study addresses aspects of cyclic plasticity (viscoplastic CHABOCHE model), anisotropic hyperelasticity (Kaliske's model), isotropic damage in hyperelastic materials (OGDEN-ROXBURGH MULLINS-effect model), and the nonlinear cyclic viscoelasticity of filled elastomers (BERGSTRÖM-BOYCE model).

Particular attention is given to practical, low-scale physical mechanisms (micromechanisms) underlying the formulations of these constitutive frameworks. In an effort to expand the applicability of these material models to modern product design, a unified family of methods and tools for identification of associated material parameters is presented.

The goal of this series of contributions is to illustrate, via carefully crafted material benchmarks, how ANSYS Mechanical APDL can easily perform quantitatively correct simulations of the nonlinear mechanical response of many types of engineering materials.

Introduction
Constitutive equations characterizing material responses are essential for any structural or mechanical calculation. The functional form of these relations can vary, from linear in the case small-strain elastic structural analyses (HOOKE's law) to complex nonlinear in the case of inelastic analysis of rate-dependent material responses with hysteresis (cyclic plasticity).

This study considers only the conventional *continuum* (or phenomenological) approach to cyclic plasticity. This approach is equivalent to averaging out the local structural effect of microstructural heterogeneity in the stress and strain fields within a representative portion of the material (a periodic mesoscopic polycrystal), and considering it only indirectly via the introduction of *internal* variables. The micromechanical motivation underlying the selection and interpretation of these internal variables is also acknowledged.

Constitutive modeling of cyclic plasticity and viscoplasticity has developed markedly over the past three decades. On the basis of the BESSELING's [1] multilayer model, MROZ [2] advanced his renowned multisurface model, inspiring several other plasticity formulations unified by the concept of bounding surfaces in the stress space. [3]

The nonlinear kinematic hardening rule on which the model outlined is based (Equation (6)) was originally proposed by ARMSTRONG and FREDERICK in 1966 [4]. By combining, in a single mathematical framework, creep and rate-independent plasticity, BODNER and PARTOM laid down the foundation of unified cyclic viscoplasticity modeling in 1972.

Further constitutive theories based on the same concepts were proposed in the mid-1970s through the early 1980s for the velocity-(rate-) dependent plastic behavior of metal materials [5] [6].

The current state of the art in cyclic plasticity phenomenological modeling involves either the multisurface conceptual view of MROZ or treating cyclic plasticity from the unifying perspective advanced by BODNER and PARTOM. The most recent progress elaborates and improves upon these modeling frameworks to simulate the physical phenomenon of ratcheting strain accumulation (or simply ratcheting).

By ratcheting, the plastic deformation occurring during cyclic loading is typically not fully reversed after unloading, and this effect is compounded during successive cycles. Depending on the circumstances, ratcheting may slow down and stop, continue at a constant rate, or accelerate. If ratcheting slows down and stops, it is referred to as *plastic shakedown*. A typical ratcheting effect is observed in clock mainsprings which, after a long period of use, relax and no longer provide sufficient power to drive the clock mechanism.

More detail is provided below concerning the capabilities of the unified viscoplastic framework proposed by J.L. CHABOCHE and available in ANSYS Mechanical 12.0 for simulating cyclic plasticity with ratcheting.

This paper has the following structure:

- A brief review of cyclic plasticity micromechanics is presented.
- The essential features of the Chaboche viscoplastic model are noted, with particular attention directed to the form of the dynamic recovery function and the physical interpretation of the back-stress multikinematic law.
- The capabilities of the model are briefly illustrated, and cyclic viscoplasticity simulation results for the AISI 316H specimen are provided.
- A brief description is given of the curve-fitting tool developed by CADFEM for estimating material parameters in the multikinematic law.

Motivation
Besides the clock mainspring scenario, another classic case where ratcheting strain accumulation can be observed is the nuclear re-

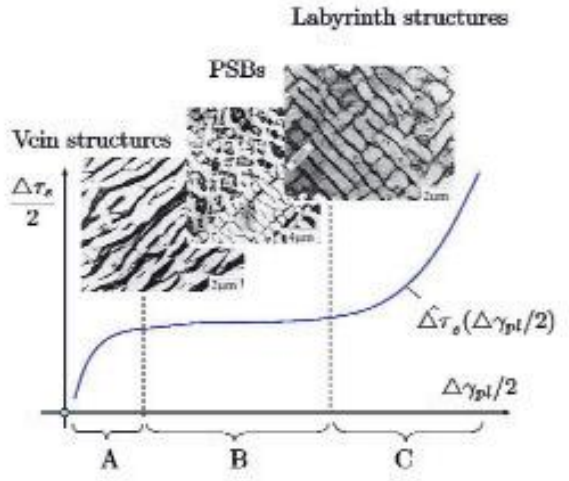

Figure 1: Cyclic stress–strain curve (amplitude of the resolved saturation shear stress $\Delta\tau_s/2$ vs. the plastic-shear amplitude $\Delta\gamma_{pl}/2$) for typical single crystal. Different dislocation structures develop during the increase of $\Delta\gamma_{pl}/2$: In range A) vein structures are observed, range B) is characterized by nucleation of PSBs from the dissolved veins; and finally range C) is characterized by labyrinth microstructures.

Figure 1: Cyclic stress-strain curve

actor mantel. The typical nuclear reactor mantel is made of austenitic stainless steels and undergoes large variety of time-dependent stress-strain histories during its service time. As a consequence, three general response types emerge in the mantel on the level of each of its material points:

- *Incremental collapse*
  Characterized by an increase of the mean stress curve, up to fracture.
- *Low-cycle fatigue*
  Occurs with a constant mean stress.
- *Elastic vibrations* (also known as *elastic shakedown*)
  Appears as a consequence of a corresponding decrease in amplitudes of plastic strain vibrations. The stress response of particular material point therefore enters the elastic region (that is, the domain enclosed by the yield surface in the stress space), while the plastic saturation displayed by *universal* flow-curve diagrams (as shown in see Figure 3) indicates ratcheting.

Introduction to the micromechanics of cyclic deformation in crystal grains and metallic polycrystals

Both deformation-induced dislocation activities in the crystal grains of a polycrystal and the micromechanics of deformation share certain similarities; however, the general nature of dislocation activity in a crystal grain during cyclic deformation is different compared to that occurring during a monotonic deformation process.

Thus far, it is known that the cyclic deformation at the grain level is characterized by an approximately equal number of positive and negative dislocations. As a result, no long-range internal stresses develop and cyclic hardening is attributed to both the attractive interactions and dislocation locking by dipole formations.

The dislocation dipoles arrange themselves into specific dissipative structures at low plastic shear strain amplitudes, as shown by (A) in Figure 1. These structures are called *dislocation veins*.

A further increase of the number of cycles, results first in an increase in the dislocation density within the veins, followed by increase in the fraction of veins per unit volume of the deformed material.

In Stage B, the resolved shear stress at the cyclic saturation remains almost constant – a plateau appears – when the plastic strain amplitude is increased. The effect is attributed to the formation of *persistent slip bands* (PSBs). Within PSBs, plastic deformation is approximately 100 times higher than within the vein-structured surroundings.

The plastic saturation state within the PSBs is determined by the dynamic equilibrium between dislocation multiplications, and dislocation annihilations. The latter effect yields to a generation of vacancies, and therefore to an increase of the volume of persistent slip bands and formation of protrusions on the surface of the specimen.

The range C of plastic shear strain values further increases the saturation of the shear stress amplitude and rearranges the dislocation veins into labyrinth structures.

Perhaps the most representative manifestation of cyclic deformation in metals and alloys occurs next – the BAUSCHINGER effect, a substantial decrease of the yield stress after cyclic load reversal.

Unified continuum representation of polycristal micromechanics: aspects of unified theory of cyclic viscoplasticity

Unified in the current context means that the theory of viscoplasticity is constructed by the phenomenological combination of rate-independent, nonlinear isotropic/kinematic hardening models and viscoplastic models developed for monotonic loading cases. To better understand the basic theory, assume linear kinematics (that is, small strains) applied under cyclic loading conditions. Beginning with the rate-independent variant of the theory, we expand the complexity further to the viscoplastic case. The basic equations governing the rate-independent plastic response of material point are given in isothermal context with the system, as follows:

$$\begin{cases} \varepsilon = \varepsilon^e + \varepsilon^p, \\ \sigma \quad \mathbf{C}[\varepsilon \quad \varepsilon^p], \\ f(\sigma, \boldsymbol{X}, R) \quad \|\sigma \quad \boldsymbol{X}\| \quad k \quad R(p), \\ \dot{\varepsilon}^p = \dot{\lambda} f_{,\sigma}. \end{cases}$$ Equation (1)

The first equation is the additive decomposition of the total strain tensor ε into an elastic part ε^e, and traceless plastic part ε^p.

The second equation is the generalized HOOKE's law of linear elasticity with $\mathbf{C}$, the super-symmetric forth rank elasticity tensor.

The function f is the yield function enclosing the elastic vector states $\{\sigma, R, \boldsymbol{X}\}$. Here, σ is the CAUCHY stress, R is the stress-like isotropic hardening variable, and X is the backstress tensor.

The final expression is the flow rule, whose plastic multiplier $\dot{\lambda}$ is determined from the loading-unloading condition $\lambda \dot{f}$ 0. In case of viscoplastic behaviour (or rate-dependency), the framework given in the Equation (1) is generalized via a viscoplastic potential Ω $\Omega(f)$. The stress state σ is allowed to move outside the elasticity domain with positive values of $f > 0$; in this way f can be interpreted as a scalar measure of the (viscous) ovrstress.

The flow rule therefore modifies to:

$\dot{\varepsilon}^{p}$ $\Omega(f)_{,\sigma}$ $\Omega_{,f} f_{,\sigma}$ $\dot{p} f_{,\sigma}$ Equation (2)

where λ is replaced by the norm of the viscoplastic strain rate $\dot{p}$ $\|\dot{\varepsilon}^{p}\|$. The derivative $\Omega_{,f}$ is the viscosity function.

Equation (2) involves two essential choices:

- **The choice of the viscosity function** $\Omega_{,f}$, or the equivalent (but technically more involved) viscoplastic potential Ω, which governs the evolution of (visco)plastic strain ε^{p}.
- **The choice of the hardening rule** for internal stress-like variables (R and $\mathbf{X}$), characterizing the geometrical motion of the yield surface.
  The generic form of a hardening rule includes three terms:
  - *Strain hardening*
    The strain hardening term gives an (increasing) evolution of typical stress-like hardening variable with the plastic strain rate.
  - *Dynamic recovery*
    The dynamic recovery term gives an instantaneous recall, acting with the plastic strain.
  - *Static recovery*
    The static recovery term is usually independent of any plastic strain, and represents certain thermally activated static recovery mechanism. This term expresses the effects of the thermal agitation by dislocation multiplications as well as the effect from dislocation annihilation on the level of the single-crystal grain.

A more detailed discussion of the constitutive choices enforced by the CHABOCHE model begins with the choice of the viscosity function.

The highly nonlinear relationship between the viscous overstress and the plastic strain rate norm is approximated, within a large range of equivalent plastic strain rates, by a NORTON type of power function:

$\dot{p}$ $\left\langle \frac{f}{\eta} \right\rangle^{n}$, Equation (3)

where the familiar MCCAULEY brackets designate that within the elastic domain in the generalized stress space, there is no accumulation of plastic strain (that is, $\dot{p}$ identically vanishes there).

The next class of equations concerns the second essential choice, the *evolution law for the isotropic hardening state* (that is, the evolution law for the size of the elastic domain).

Notice first that with Equation (1) (expression 3), Equation (3) can be expressed as follows:

$\dot{p}$ $\left\langle \frac{\|\sigma \quad X\| \quad k}{K} \quad R(p) \right\rangle^{n}$, Equation (4)

Equation (4) suggests three possibilities for introducing the isotropic hardening:

- Through explicit expression for stress-like variable R
- By an increase of the viscosity parameter K
- By coupling p with the evolution law for X

In the first two cases, one needs to define the one-to-one relationship between R (or K) and the accumulated plastic strain p (strain-hardening) or plastic work W^{p} (work-hardening). An example of the evolution law for R is given in Equation (7) below.

Finally, the kinematic type of hardening is typical for moderate strain applications. Its activation is motivated by either non-proportional types of monotonic loading or cyclic loading (where several load reversals are present).

Linear relationships, such as the PRANDTL kinematic hardening rule, provide a relatively bad quantitative account of this type of hardening response. A better description is given by the non-linear model of ARMSTRONG and FREDERICK [4], which contains a dynamic recovery term $\gamma \mathbf{X} \dot{p}$, and is given by:

$$\dot{\mathbf{X}} = \frac{2}{3} C \dot{\varepsilon}^{p} - \gamma \mathbf{X} \dot{p}, \qquad \text{Equation (5)}$$

In this equation, C and γ are two material parameters. The recall term is co-linear with X and is proportional to $\dot{p}$. The evolution of the back-stress tensor, is therefore exponential for piecewise smooth monotonic uniaxial loading application and saturates at C/γ.

Further improvement of the predictions from this non-linear kinematic hardening rule has been realized with a modification proposed by CHABOCHE [6]. In essence, this modification consists of an additive superposition of several models similar to Equation (5), whose dynamic recovery constants differ by several orders of magnitude, as shown

$\dot{\mathbf{X}}$ $\sum_{i=1}^{m} \dot{\mathbf{X}}_{i}$ $\sum_{i=1}^{m} \frac{2}{3} C_{i} \dot{\varepsilon}^{p}$ $\gamma_{i} \mathbf{X}_{i} \dot{p}$. Equation (6)

Equation (6) expands the functionality of ARMSTRONG-FREDERICK model to larger strain ranges and provides better descriptions of the soft transition between elasticity and the onset of plastic flow. The parameters introduced by such superposition of backstresses are interpreted as coefficients of a finite series representation of the multikinematic hardening rule. This interpretation is also justified in the context of the endochronic plasticity theory.

Example

Consider this example of the CHABOCHE viscoplastic constitutive framework to predict the ratcheting in a rectangular block made of AISI 316H austenitic stainless steel [7]. The boundary conditions are shown in Figure 2. On one pair of sides, the steel block is loaded by constant normal stress field, whereas four of the lateral sides undergo harmonically changing system of balanced

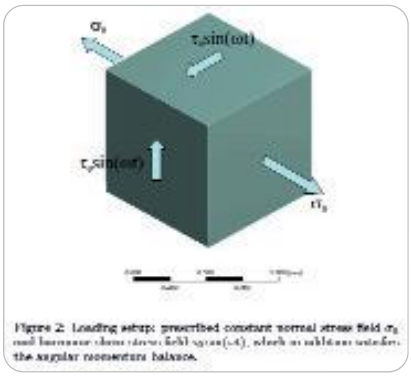

Figure 2: Loading setup

shear stresses. It is experimentally observed that such temporal variation of applied load induces a progressive but saturated increase of the axial strain co-linear with the normal stress components. The strain rate is of the order of 0.001 s^{-1}.

For the simulation, the normal stress field is set to σ_T = 245 MPa, while the harmonic shear stress is characterized by $\tau = \tau_0 \sin(\omega t)$ with amplitude τ_0 75 MPa and frequency frequency ω 11.5 rad/s.

The choice of loading parameters is consistent with the experimental data set reported by MICUNOVIC. [7] The particular form of the CHABOCHE viscoplastic model contains single-mode kinematic hardening law and exponential isotropic hardening law,

$$\begin{cases} \dot{\varepsilon}^p = \left\langle \frac{\|\sigma - X\| - R}{K} \right\rangle^m \frac{\sigma - X}{\|\sigma - X\|}, \\ \dot{X} = \frac{2}{3} C \dot{\varepsilon}^p - \gamma X \dot{p}, \\ \dot{R} = b(R_\infty - R)\dot{p}. \end{cases}$$

Equation (7)

The results obtained from the numerical integration of this model are shown in Figure 3.

Identification of material parameters for the non-linear kinematic hardening part

The most challenging task when identifying material parameters for (7) involves estimating nonlinear kinematic hardening constants in the ARMSTRONG-FREDERICK rule.

On the basis of two-load reversal uniaxial stress-strain cycle, CADFEM developed a curve-fitting tool to calibrate up to five ARMSTRONG-FREDERICK kinematic models (with up to 12 material constants including the yield stress and YOUNG's modulus), superimposed in the form proposed by CHABOCHE. The tool is based on computational minimization of the least-square error between predicted and measured uniaxial stress values.

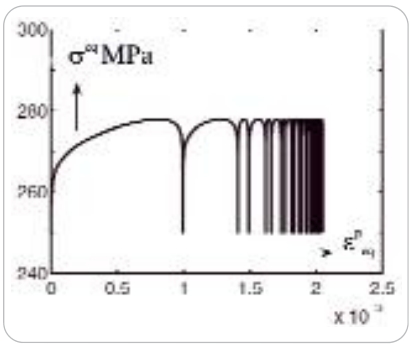

Figure 3: Ratcheting strain accumulation observed in the so square error with recalled universal flow curve (equivalent stress vs. accumulated plastic strain). See also [7 (p. 197].

From an algorithmic perspective, the curve-fitting tool uses the NELDER-MEAD simplex method for estimating the derivatives from the least-square error with respect to material constants. At each iteration step, the method is combined at with an explicit integration strategy for the uniaxial version of the nonlinear kinematic hardening model (Equation (6)). Screenshots from a typical session with CFT are shown in Figures 4 and 5.

Fig. 4: Graphical user interface of CHABOCHE curve-fitting tool (CFT): shown are the adjustment sliders for the material integration solver and least-square minimization algorithm, as well as data import button.

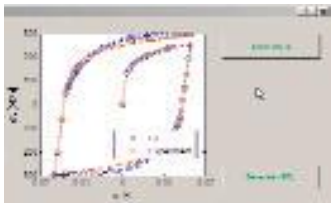

Figure 5: Graphical user interface of CFT with fit of uniaxial response data set..

The experimental data set necessary for estimating the material parameters is provided in ASCII format. Finally, the curve-fitting tool offers visual control of the quality of the fit, as well as automatic generation of the APDL code segment for the CHABOCHE nonlinear kinematic hardening model. <<

Author

Dr. Slav Dimitrov, CADFEM GmbH Grafing
Tel. +49 (0) 80 92-70 05-40
E-Mail sdimitrov@cadfem.de

References

[1] BESSELING, J.M. (1958). *A theory of elastic, plastic and creep deformations of an initially isotropic material showing anisotropic strain hardening, creep recovery and secondary creep.* ASME J. Appl. Mech. 25, p.529 – 536.

[2] MROZ, Z. (1967). *On the description of anisotropic work hardening.* J. Mech. Phys. Solids 15, p.163 – 175.

[3] DEFALIAS, Y.P., and E.P. POPOV (1976). *Plastic internal variables formalism of cyclic plasticity.* ASME J. Appl. Mech. 45, p.645 – 651.

[4] ARMSTRONG, P.J. and C.O. FREDERICK (1966). *A mathematical representation of the multiaxial Bauschinger effect.* Report RD/B/N731, CEGB, Central Electricity Generating Board, Berkeley, UK.

[5] CHABOCHE, J.L. (1989). *Constitutive equations for cyclic plasticity and cyclic viscoplasticity.* Int. J. Plasticity 5, p.247 – 302.

[6] CHABOCHE, J.L. (2008). *A review of some plasticity and viscoplasticity theories.* Int. J. Plasticity 24, p.1642 – 1693.

[7] MICUNOVIC, M.V. (2009). *Thermomechanics of viscoplasticity: fundamentals and applications.* Advances in Mechanics and Mathematics 20, Springer.